Comparison of *N*-acetyl-glucosamine to other monosaccharides reveals structural differences for the inhibition of α-synuclein aggregation

Ana Galesic[#1], Ananya Rakshit[#1], Giuliano Cutolo[1], Ricardo Palos Pacheco[1], Aaron T. Balana[1], Stuart P. Moon[1], Matthew R. Pratt[1,2,3]

[1]Department of Chemistry, University of Southern California, Los Angeles, CA 90089, United States

[2]Department of Biological Sciences, University of Southern California, Los Angeles, CA 90089, United States

[#] These authors contributed equally to this work.

Abstract

O-GlcNAc modification of tau and α-synuclein can directly inhibit the formation of the associated amyloid fibers associated with major classes of neurodegenerative diseases. However, the mechanism(s) by which this posttranslational modification inhibits amyloid aggregation are still murky. One hypothesis is that O-GlcNAc simply acts as a poly-hydroxylated steric impediment to the formation of amyloid oligomers and fibers. Here, we begin to test this hypothesis by comparing the effects of O-GlcNAc to other similar monosaccharide - glucose, N-acetyl-galactosamine (GalNAc), or mannose - on α-synuclein amyloid formation. Interestingly, we find that this quite reasonable hypothesis is not entirely correct. More specifically, we used four types of biochemical and biophysical assays to discover that the different sugars display different effects on the inhibition of amyloid formation, despite only small differences between the structure of the monosaccharides. These results further support a more detailed investigation into the mechanism of amyloid inhibition by O-GlcNAc and has potential implications for the evolution of N-acetyl-glucosamine as the monosaccharide of choice for widespread intracellular glycosylation.

INTRODUCTION

O-GlcNAc modification is the dynamic addition of the N-acetylglucosamine to serine and threonine residues of intracellular proteins (Figure 1a) and appears to play multiple important roles in the inhibition of neurodegenerative diseases.[1] For example, direct O-GlcNAc modification of the amyloid-forming proteins tau and α-synuclein inhibits their

aggregation *in vitro*. Additionally, a small molecule inhibitor of the enzyme that removes O-GlcNAc, O-GlcNAcase (OGA), increases overall modification levels, slows neurodegeneration in mouse models of Alzheimer's disease,[2,3] increases autophagy,[4] and inhibits the uptake and toxicity of α-synuclein amyloid fibers in primary neurons.[5] Conversely, conditional knockout of the enzyme that adds O-GlcNAc, O-GlcNAc transferase (OGT), in mouse forebrains leads to neurodegeneration.[6] Finally, multiple studies have found that O-GlcNAc is lower in Alzheimer's disease patients compared to age-matched controls.[7–9]

Our own work in this area has focused on the major amyloidogenic protein in Parkinson's disease, α-synuclein. α-Synuclein (Uniprot: P37840) is a short, 140 amino acid protein found at relatively high concentrations (~50 μM) at pre-synaptic termini.[10,11] This protein is natively unstructured in solution but can form an α-helix on the surface of lipid vesicles where it participates in membrane remodeling and vesicle trafficking. Unfortunately, α-synuclein can also form toxic amyloid oligomers and fibers. These fibers can then spread from cell to cell resulting in the progressive loss of dopaminergic neurons and the onset of Parkinson's disease symptoms. Proteomic analysis from human and mouse tissue has found α-synuclein to be O-GlcNAc modified at nine different positions (Figure 1b).[12,13] OGT does not display a strong primary sequence dependence but does prefer unstructured regions of proteins. Therefore, it is not necessarily surprising that a natively unfolded protein like α-synuclein could be this broadly modified. To understand the consequences of O-GlcNAc on α-synuclein aggregation, we employ synthetic protein chemistry to prepare site-specifically and homogeneously modified protein for biological studies. Specifically, we take advantage of expressed protein ligation (EPL) to combine synthetic and recombinant protein fragments (Figure 1b).[14] α-Synuclein contains no native cysteines require for the ligation reactions, but we can simply introduce cysteine in the place of any of the numerous alanine residues and subject them to desulfurization at the end of the synthesis.[15] Using this synthetic strategy, we previously described the preparation and characterization of six different O-GlcNAc modified variants of α-synuclein.[16–18] We found that all of the O-GlcNAc modifications inhibit at least the kinetics of α-synuclein aggregation and several appear to affect the structure of any amyloid fibers that do form, suggesting that increasing O-GlcNAc might be a therapeutic strategy to slow the progression of Parkinson's disease.

During the course of describing these results, we have been often asked if any monosaccharide would result in slower aggregation, as the simplest hypothesis to explain O-GlcNAc's ability to inhibit amyloid formation is that it is acting as a relatively hydrophilic, steric block. If this is true, one would expect that many similarly structured monosaccharides would behave in the same fashion. Here, we test this possibility through the synthesis of four different α-synuclein proteins bearing O-GlcNAc, β-*O*-GalNAc, β-*O*-glucose, or α-*O*-mannose at threonine 72 (Figure 1c). We then used a variety of biochemical techniques to determine the effects of the different monosaccharides on amyloid aggregation. Consistent with our previous publications, O-GlcNAc at threonine 72 strongly inhibited α-synuclein aggregation. Interestingly, we found that despite only small differences in their structures, the other monosaccharides had different effects on inhibition. This suggests that O-GlcNAc is not simply functioning as a generic hydrophilic moiety, with interesting implications for the evolution of this type of glycosylation.

RESULTS AND DISCUSSION

We chose the β-*O*-GalNAc and β-*O*-glucose monosaccharides as they provide a limited structural activity relationship profile of the O-GlcNAc, and we picked α-*O*-mannose because it has been shown to potentially be a replacement for O-GlcNAc in *Sacchromyces cerevisiae*.[19] We performed a stepwise assembly of three protein fragments (Supporting Information, Figures S1–S3) to yield the final glycosylated proteins (Figure 2a). We first synthesized the glycosylated threonine building-blocks using our InBr$_3$ catalyzed glycosylation.[20] This was followed by standard Fmoc-based solid phase peptide synthesis on hydrazine resin resulting C-terminal hydrazide peptides (**1**-**4**). We then reacted these peptides with a recombinant thioester protein **5** (Figure S4), which was previously expressed as an intein fusion. The C-terminal hydrazides were then transformed to the corresponding thioesters[21] and reacted the N-terminal cysteine protein **6** (Figure S5), which we expressed recombinantly in *E. coli* by taking advantage of its endogenous methionine aminopeptidase. Finally, we removed the acetate protecting groups from the monosaccharides (Figure S6) took advantage of desulfurization chemistry to transform the cysteines required for the ligation reactions back to their native alanines in the α-synuclein primary sequence (Figure S7). The final protein products, α-synuclein(GlcNAc), (Glc), (GalNAc), and (Man), were characterized by RP-HPLC and mass spectrometry (Figure 2b). We then subjected the soluble proteins to analysis by circular dichroism (CD) and dynamic light scattering (DLS), and we found that all proteins were essentially identical to unmodified, recombinant α-synuclein, unfolded in solution (Figure S8), and monomeric in size (Figure S9).

With these proteins in hand, we next moved to examine how they affect the amounts of α-synuclein aggregation using three methods: Thioflavin T (ThT) fluorescence, dot-blotting, and proteinase K (PK) digestion. We first subjected all four modified proteins, as well as unmodified recombinant α-synuclein, to aggregation conditions (50 μM protein concentration, agitation at 1,000 rpm, and 37 °C) in phosphate buffer (pH 7.4) for 7 days (168 h). Aliquots of the reaction mixture were removed after 48, 96, and 168 h, mixed the ThT, and analyzed by plate reader (Figure 3a). ThT is a member of environmentally sensitive dyes that display increased fluorescence in the presence of amyloid fibers due to interpolation of the dye into hydrophobic grooves that form along the side of the aggregates. As expected from our previous results,[18] unmodified α-synuclein rapidly aggregated over the course of the assay, while α-synuclein(GlcNAc) displays slower aggregation kinetics and lower overall ThT signal at the end of the assay. All three of the other monosaccharides also displayed lower ThT signals, indicating reduced formation of α-synuclein aggregates. Notably, however, α-synuclein(Man) appeared to be more inhibitory than α-synuclein(Glc) or α-synuclein(GalNAc). We next analyzed the aggregation reactions at the end of the assay (168 h) by dot-blotting with an antibody (A17183A) that broadly recognizes α-synuclein amyloid aggregates, including oligomers and fibers (Figure 3b). We quantitated the signal from the dot blot and found that the results were consistent with the ThT measurements, with all four glycosylated proteins showing fewer amyloids and α-synuclein(GlcNAc)/α-synuclein(Man) having the least. Next, we subjected the 168 h reaction mixtures to digestion by PK (Figure 3c). PK is a highly promiscuous protease that will completely digest monomeric α-synuclein. However, certain amyloid structures restrict the access of PK to the

internal segments of α-synuclein, resulting in stable bands that can be visualized by SDS-PAGE. This banding pattern gives a low resolution picture of qualitative differences in the amyloid structure.[22] Because the digestion is performed on the entire aggregation reaction, a mixture of monomers, oligomers, and fibers, it can also be used as a proxy for aggregate stability. Specifically, the proteolysis of full-length α-synuclein corresponds to the amount of aggregation and the stability of those amyloids. For unmodified α-synuclein, we observed stability of the full-length band and five overall bands in the pattern observed for "typical" stable amyloid-fibers. Similar to our published results, we found much less full-length protein upon digestion of α-synuclein(GlcNAc) and a three-band pattern. Despite the relatively high signal from ThT fluorescence and dot-blotting, we observed essentially complete degradation of α-synuclein(GalNAc) by PK. We found that digestion of both α-synuclein(Glc) and α-synuclein(Man) resulted in three bands that are similar to α-synuclein(GlcNAc). However, those bands had different stabilities depending on the monosaccharide. Finally, we separated the soluble protein from any aggregate pellets by centrifugation and analyzed the relative amounts of protein by SDS-PAGE and staining (Figure 3d). These results were in good agreement with both the ThT and dot-blotting data, confirming that all four of the monosaccharides inhibit the overall amount of aggregation. Specifically, α-synuclein(GlcNAc) and α-synuclein(Man) showed similar and lower levels of protein in the pellet, followed by α-synuclein(Glc) and α-synuclein(GalNAc), also with essentially the same aggregate amounts.

Next, we set out to confirm our results by repeating the aggregation reactions. However, this time we extended the timeframe of the aggregation to potentially accentuate any differences between the different monosaccharides. Overall, we observed results that were very consistent with the previous set of experiments. ThT fluorescence showed that all of the different sugars inhibited the kinetics of α-synuclein aggregation, and that α-synuclein(GlcNAc)/α-synuclein(Man) were more inhibitory (Figure S10a). Notably, at the extended timepoint of this assay (192 h), we found that α-synuclein(GalNAc) displayed more ThT signal than α-synuclein(Glc) (Figure S10a). Dot-blotting once again largely confirmed these results (Figure S10b). We also analyzed the 192 h reaction mixture by PK digestion (Figure S10c). Once again, digestion of α-synuclein(GlcNAc) and α-synuclein(GalNAc) resulted in almost no detectable stable bands. As expected from the longer aggregation, and therefore more amyloid formation, we observed more stable bands for both α-synuclein(Glc) and α-synuclein(Man). We attribute the differences between the results in Figure 3 and Figure S10 to result from the additional aggregation time resulting in generally higher ThT levels and more stable PK digestion patterns.

Finally, we analyzed the 192 h timepoint from this second aggregation reaction by transmission electron microscopy to characterize the structure of the any amyloids that formed (Figure 4 & S11). As expected from our prior work,[18] unmodified α-synuclein formed long fibers consistent with typical amyloids, while α-synuclein(GlcNAc) only yielded short and broken fiber structures. α-Synuclein(Glc) and α-synuclein(GalNAc) both formed long amyloid fibers more similar to unmodified α-synuclein than α-synuclein(GlcNAc). Finally, we found a mixture of both long fibers and short, broken structures formed by α-synuclein(Man).

Taken together, our results yield some interesting and somewhat expected conclusions. O-GlcNAc is the only monosaccharide tested that strongly inhibits the amyloid aggregation of α-synuclein using all four different characterization techniques: ThT fluorescence, dot-blotting, PK digestion, TEM imaging. On the other end of the spectrum, we found that glucose modification was the least inhibitory, with relatively high ThT fluorescence and dot-blot signal attributable to amyloid oligomers and/or fibers, as well as significant protein in the insoluble pellet and several bands that were stable to PK digestion and long fibers visualized by TEM. We found intermediate results for both α-synuclein(GalNAc) and α-synuclein(Man). In the case of α-synuclein(GalNAc), the ThT fluorescence, dot-blotting, and TEM all showed the formation of notable amounts of long amyloid fibers. This was accompanied by a large fraction of protein in the insoluble pellet. However, these aggregates were not stable to PK digestion. Interestingly, these results are consistent with a recent report on α-synuclein "needles" that are a structurally different polymorph of the α-synuclein amyloid.[23] We believe that GalNAc at T72 may be inducing the formation of needles, or something similar, instead of the more traditional fiber amyloid structure. There is precedent for PTMs causing different α-synuclein polymorphs, including our own work on O-GlcNAc at serine 87[18] and phosphorylation at tyrosine 39.[24] Finally, α-synuclein(Man) gave ThT, dot-blot, and insoluble aggregate signals that were similar to α-synuclein(GlcNAc), α-synuclein(Man) also yield a mixture of broken and long amyloids visualized by TEM that were at least partially stable to PK digestion. It is possible that mannose is also forcing the formation of a polyform, but we are not aware of any previously characterized amyloid that share these characteristics. α-Synuclein(Man) may display a more bifurcated aggregation process that results in a mixture of small, broken structures similar to α-synuclein(GlcNAc) and longer amyloids. Notably, unlike the other sugars, the mannose monosaccharide is attached through an α-linkage, potentially explaining its unique consequences.

Currently there is no physiological relevance to modification of α-synuclein by glucose, GalNAc, or mannose, as these modifications have never been observed. At the outset of these experiments, we assumed that any monosaccharide would function similarly by acting as a hydrophilic, steric impediment to the formation of the largely hydrophobic core of the amyloid aggregate. That appears not to be the case, and small changes to the structure of the monosaccharide can have consequences. These data demonstrate that O-GlcNAc might particularly effective at inhibiting amyloid aggregation. However, we do not know if the same inhibitory trend would hold for another amyloid-forming protein or even another modification site on α-synuclein. Despite these unknowns, our results suggest that not all monosaccharides are equal inhibitors of protein aggregation with interesting implications for the evolution of this O-GlcNAc over other potential monosaccharides.

METHODS

A complete description of the experimental methods is provided in the Supporting Information.

Supplementary Material

Refer to Web version on PubMed Central for supplementary material.

ACKNOWLEDGMENTS

REFERENCES

(1). Yang X, and Qian K (2017) Protein O-GlcNAcylation: emerging mechanisms and functions. Nat Rev Mol Cell Biol 18, 452–465. [PubMed: 28488703]

(2). Borghgraef P, Menuet C, Theunis C, Louis JV, Devijver H, Maurin H, Smet-Nocca C, Lippens G, Hilaire G, Gijsen H, Moechars D, and Van Leuven F (2013) Increasing brain protein O-GlcNAc-ylation mitigates breathing defects and mortality of Tau.P301L mice. PLoS ONE 8, e84442. [PubMed: 24376810]

(3). Yuzwa SA, Shan X, Jones BA, Zhao G, Woodward ML, Li X, Zhu Y, McEachern EJ, Silverman MA, Watson NV, Gong C-X, and Vocadlo DJ (2014) Pharmacological inhibition of O-GlcNAcase (OGA) prevents cognitive decline and amyloid plaque formation in bigenic tau/APP mutant mice. Mol Neurodegener 9, 42. [PubMed: 25344697]

(4). Zhu Y, Shan X, Safarpour F, Erro Go N, Li N, Shan A, Huang MC, Deen M, Holicek V, Ashmus R, Madden Z, Gorski S, Silverman MA, and Vocadlo DJ (2018) Pharmacological Inhibition of O-GlcNAcase Enhances Autophagy in Brain through an mTOR-Independent Pathway. ACS Chem. Neurosci 9, 1366–1379. [PubMed: 29460617]

(5). Tavassoly O, Yue J, and Vocadlo DJ (2020) Pharmacological inhibition and knockdown of O-GlcNAcase reduces cellular internalization of α-synuclein preformed fibrils. The FEBS journal.

(6). Wang AC, Jensen EH, Rexach JE, Vinters HV, and Hsieh-Wilson LC (2016) Loss of O-GlcNAc glycosylation in forebrain excitatory neurons induces neurodegeneration. Proc Natl Acad Sci USA 113, 15120–15125. [PubMed: 27956640]

(7). Liu F, Iqbal K, Grundke-Iqbal I, Hart G, and Gong C (2004) O-GlcNAcylation regulates phosphorylation of tau: a mechanism involved in Alzheimer's disease. Proc Natl Acad Sci USA 101, 10804–10809. [PubMed: 15249677]

(8). Liu F, Shi J, Tanimukai H, Gu J, Grundke-Iqbal I, Iqbal K, and Gong CX (2009) Reduced O-GlcNAcylation links lower brain glucose metabolism and tau pathology in Alzheimer's disease. Brain 132, 1820–1832. [PubMed: 19451179]

(9). Pinho TS, Correia SC, Perry G, Ambrósio AF, and Moreira PI (2019) Diminished O-GlcNAcylation in Alzheimer's disease is strongly correlated with mitochondrial anomalies. BBA - Molecular Basis of Disease 1865, 2048–2059. [PubMed: 30412792]

(10). Lashuel HA, Overk CR, Oueslati A, and Masliah E (2013) The many faces of α-synuclein: from structure and toxicity to therapeutic target. Nat Rev Neurosci 14, 38–48. [PubMed: 23254192]

(11). Wilhelm BG, Mandad S, Truckenbrodt S, Kröhnert K, Schäfer C, Rammner B, Koo SJ, Claßen GA, Krauss M, Haucke V, Urlaub H, and Rizzoli SO (2014) Composition of isolated synaptic boutons reveals the amounts of vesicle trafficking proteins. Science 344, 1023–1028. [PubMed: 24876496]

(12). Wang Z, Udeshi ND, O'Malley M, Shabanowitz J, Hunt DF, and Hart GW (2010) Enrichment and Site Mapping of O-Linked N-Acetylglucosamine by a Combination of Chemical/Enzymatic Tagging, Photochemical Cleavage, and Electron Transfer Dissociation Mass Spectrometry. Mol Cell Proteomics 9, 153–160. [PubMed: 19692427]

(13). Morris M, Knudsen GM, Maeda S, Trinidad JC, Ioanoviciu A, Burlingame AL, and Mucke L (2015) Tau post-translational modifications in wild-type and human amyloid precursor protein transgenic mice. Nat Neurosci 18, 1183–1189. [PubMed: 26192747]

(14). Muir TW, Sondhi D, and Cole PA (1998) Expressed protein ligation: a general method for protein engineering. Proc Natl Acad Sci USA 95, 6705–6710. [PubMed: 9618476]

(15). Wan Q, and Danishefsky SJ (2007) Free-radical-based, specific desulfurization of cysteine: a powerful advance in the synthesis of polypeptides and glycopolypeptides. Angew Chem Int Ed Engl 46, 9248–9252. [PubMed: 18046687]

(16). Marotta NP, Lin YH, Lewis YE, Ambroso MR, Zaro BW, Roth MT, Arnold DB, Langen R, and Pratt MR (2015) O-GlcNAc modification blocks the aggregation and toxicity of the protein α-synuclein associated with Parkinson's disease. Nat Chem 7, 913–920. [PubMed: 26492012]

(17). Lewis YE, Galesic A, Levine PM, De Leon CA, Lamiri N, Brennan CK, and Pratt MR (2017) O-GlcNAcylation of α-Synuclein at Serine 87 Reduces Aggregation without Affecting Membrane Binding. ACS Chem Biol 12, 1020–1027. [PubMed: 28195695]

(18). Levine PM, Galesic A, Balana AT, Mahul-Mellier A-L, Navarro MX, De Leon CA, Lashuel HA, and Pratt MR (2019) α-Synuclein O-GlcNAcylation alters aggregation and toxicity, revealing certain residues as potential inhibitors of Parkinson's disease. Proc Natl Acad Sci USA 116, 1511–1519. [PubMed: 30651314]

(19). Halim A, Larsen ISB, Neubert P, Joshi HJ, Petersen BL, Vakhrushev SY, Strahl S, and Clausen H (2015) Discovery of a nucleocytoplasmic O-mannose glycoproteome in yeast. Proc Natl Acad Sci USA 112, 15648–15653. [PubMed: 26644575]

(20). De Leon CA, Lang G, Saavedra MI, and Pratt MR (2018) Simple and Efficient Preparation of O- and S-GlcNAcylated Amino Acids through InBr3-Catalyzed Synthesis of β- N-Acetylglycosides from Commercially Available Reagents. Org Lett 20, 5032–5035. [PubMed: 30088936]

(21). Flood DT, Hintzen JCJ, Bird MJ, Cistrone PA, Chen JS, and Dawson PE (2018) Leveraging the Knorr Pyrazole Synthesis for the Facile Generation of Thioester Surrogates for use in Native Chemical Ligation. Angew Chem Int Ed Engl 57, 11634–11639. [PubMed: 29908104]

(22). Luk KC, Covell DJ, Kehm VM, Zhang Bin, Song IY, Byrne MD, Pitkin RM, Decker SC, Trojanowski JQ, and Lee VM-Y (2016) Molecular and Biological Compatibility with Host Alpha-Synuclein Influences Fibril Pathogenicity. Cell Rep 16, 3373–3387. [PubMed: 27653697]

(23). Peduzzo A, Linse S, and Buell AK (2020) The Properties of α-Synuclein Secondary Nuclei Are Dominated by the Solution Conditions Rather than the Seed Fibril Strain. ACS Chem. Neurosci 11, 909–918. [PubMed: 32069013]

(24). Zhao K, Lim Y-J, Liu Z, Long H, Sun Y, Hu J-J, Zhao C, Tao Y, Zhang X, Li D, Li Y-M, and Liu C (2020) Parkinson's disease-related phosphorylation at Tyr39 rearranges α-synuclein amyloid fibril structure revealed by cryo-EM. Proc Natl Acad Sci USA 117, 20305–20315. [PubMed: 32737160]
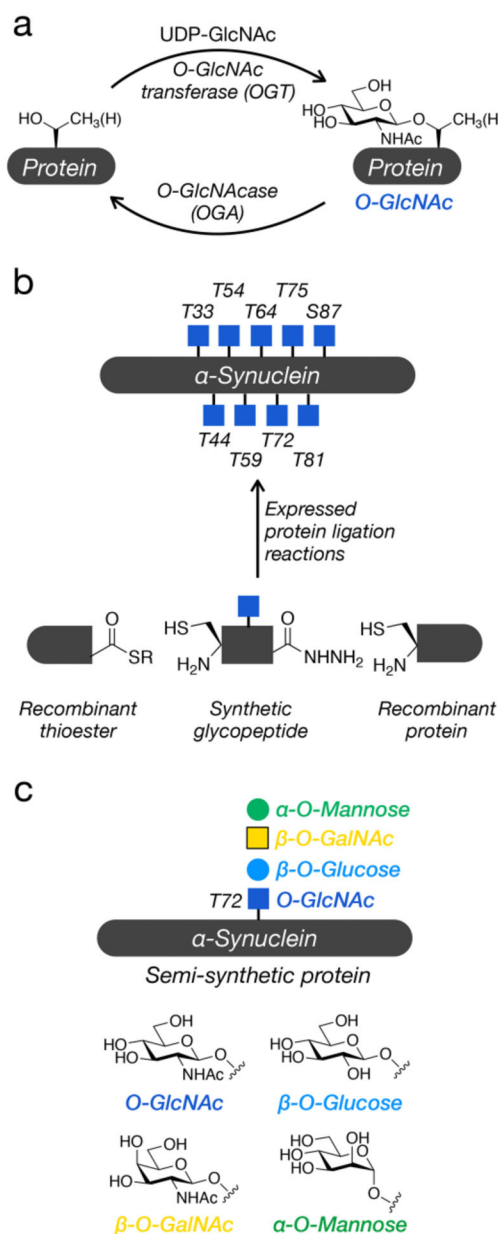
Figure 1. O-GlcNAc modification of α-synuclein.
a) O-GlcNAc is the dynamic addition of N-acetyl-glucosamine to intracellular proteins. b) α-Synuclein is modified at nine different positions with O-GlcNAc and the effects of these modifications can be studied in a site-specific fashion using protein semisynthesis. c) Here, we test the importance of O-GlcNAc for α-synuclein amyloid formation by comparing it to other monosaccharides.
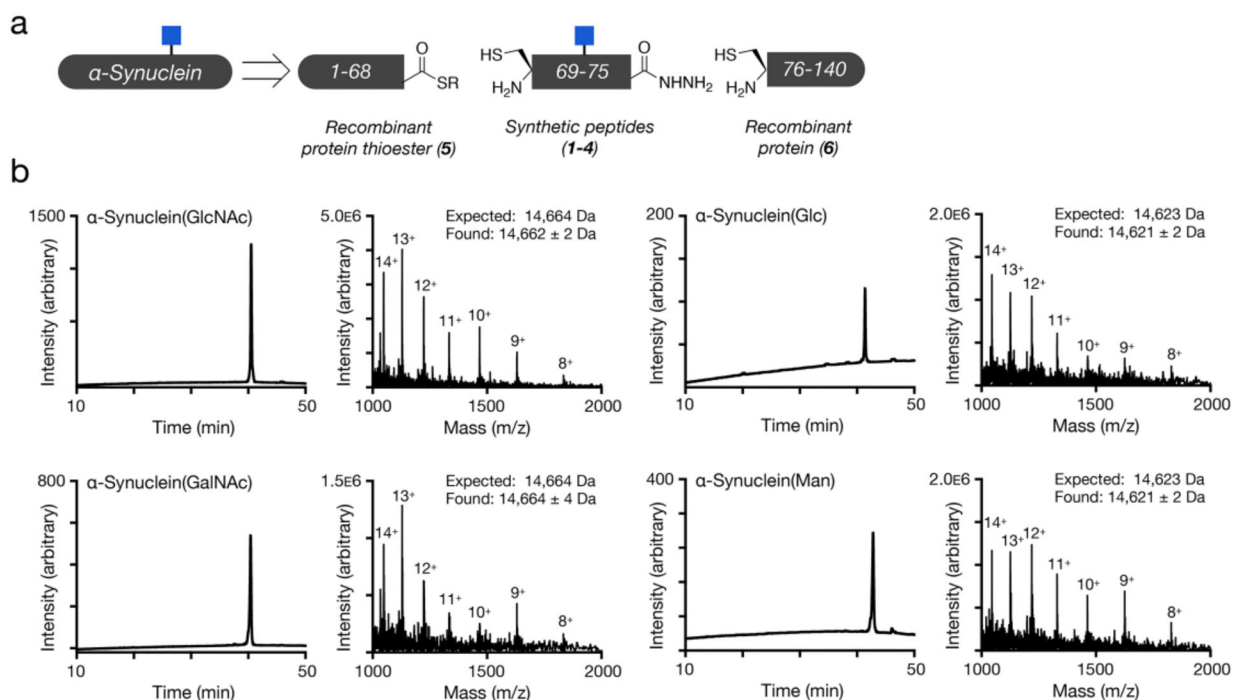
Figure 2. Synthesis and characterization of α-synuclein proteins.

a) Differentially glycosylated versions of α-synuclein were retrosynthetically deconstructed into a recombinant protein thioester, synthetic peptide thioesters prepared by solid phase peptide synthesis, and a recombinant N-terminal cysteine protein. This synthetic route is exemplified by α-synuclein(GlcNAc) b) Analytical RP-HPLC traces and ESI-MS of the indicated synthetic proteins.
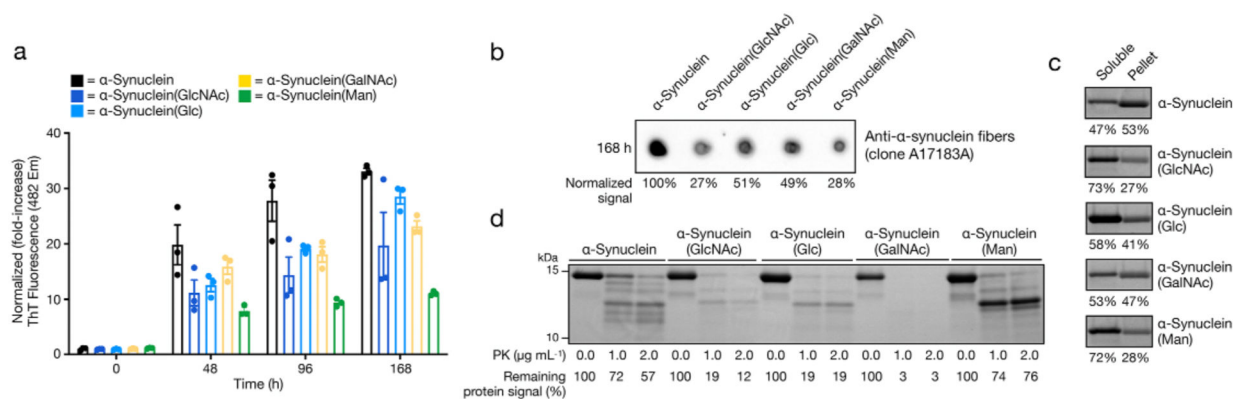
Figure 3. Different monosaccharides have distinct effects on α-synuclein aggregation.
a) Analysis of amyloid formation using thioflavin T (ThT) fluorescence (λ_{ex} = 450 nm, λ_{em} = 482 nm). The indicated α-synuclein proteins (50 μM) were subjected to aggregation conditions and analyzed by fluorescence at the indicated timepoints. b) The same reactions (168 h timepoint) were analyzed by dot-blotting using an α-synuclein amyloid-selective antibody (A17183A), and quantification was performed using ImageJ. c) The aggregation reaction mixtures (168 h timepoint) were subjected to the indicted concentrations of proteinase K (PK) before analysis by SDS-PAGE and staining with Coomassie blue. Quantification of the entire lane (10–15 kDa) was performed using ImageJ. The persistence of bands correlates with the amount and gross structure of amyloids formed. d) The soluble protein and aggregate pellets fo the reaction mixtures (168 h timepoint) were separated by centrifugation, separated by SDS-PAGE and visualized using Coomassie staining. Quantification of the major band was performed using ImageJ.
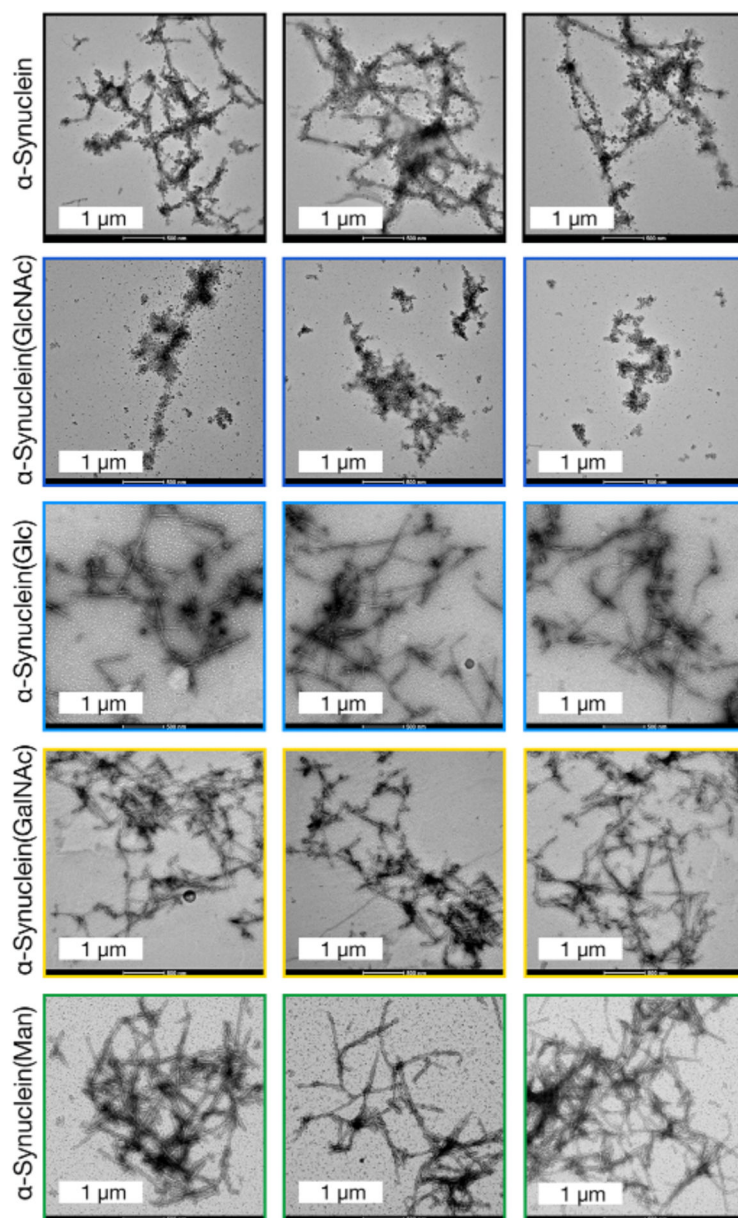
Figure 4. Analysis of the different α-synuclein aggregates using transmission electron microscopy (TEM).
The 192 h timepoint of the aggregation reactions in Figure S10 were visualized using TEM.